

SIMULATIONS OF COHERENT ELECTRON COOLING WITH ORBIT DEVIATION*

J. Ma[†], G. Wang, V. N. Litvinenko¹, Brookhaven National Laboratory, Upton, New York, USA
¹also at Stony Brook University, Stony Brook, New York, USA

Abstract

Coherent electron cooling (CeC) is a novel technique for rapidly cooling high-energy, high-intensity hadron beam. Plasma cascade amplifier (PCA) has been proposed for the CeC experiment in the Relativistic Heavy Ion Collider (RHIC) at Brookhaven National Laboratory (BNL). Cooling performance of PCA based CeC has been predicted in 3D start-to-end CeC simulations using code SPACE. The dependence of the PCA gain and the cooling rate on the electron beam's orbit deviation has been explored in the simulation studies.

INTRODUCTION

Strong hadron cooling (SHC) is essential to attain the luminosity required by the future Electron-Ion Collider (EIC) design. CeC [1-3] is a promising technique for the rapid cooling of high-energy high-intensity hadron beams in the EIC.

A CeC system consists of three main sections, the modulator, the amplifier, and the kicker. Several CeC schemes have been proposed with different implementations of the CeC amplifier. In this paper, we present simulation studies of the PCA-based CeC [4]. Working principle of PCA is the new plasma cascade instability (PCI) [5-6].

Figure 2 shows the layout of a PCA-based CeC system, where solenoids are used to modulate the transverse size of the electron beam and to excite the PCI.

Our simulation tool is the SPACE code [7], a parallel, relativistic, three-dimensional (3D), electromagnetic (EM) Particle-in-Cell (PIC) code, which has been used in the simulation studies for the mitigation effect by beam induced plasma [8], the modulation process in CeC [9-12], CeC with free electron laser (FEL) amplifier [13-16] and the CeC with PCA [17-18].

CEC WITHOUT ORBIT DEVIATION

The setup of the CeC system in the simulation study is based on the CeC experiment at BNL RHIC, which includes a 2.88-meter modulator, an 8-meter 4-cell PCA and

a 3-meter kicker. The lengths of the PCA cells are 1.8 m, 2.2 m, 2.2 m, and 1.8 m. Table 1 lists two cases of electron beam parameters in simulations. The electron beam peak current and emittance are carefully chosen to excite the PCI in PCA, and therefore amplify the density modulation introduced by ions in the modulator.

Table 1: Electron Beam Parameters

	Case 1	Case 2
Beam energy, γ	28.5	28.5
Peak current, A	50	75
Normalized KV emittance, mm mrad	6	7
RMS energy spread	2e-4	2e-4

A transverse Kapchinsky-Vladimirsky (KV) distribution has been applied to the electron beam in the simulations. Note that the KV emittance is 4 times of the traditionally defined root-mean-square (RMS) emittance.

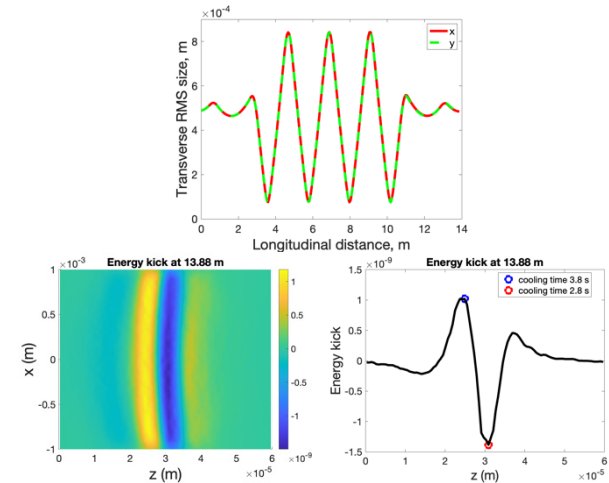


Figure 1: Evolution of transverse RMS beam size in a 4-cell-PCA based CeC system for electron beam peak current 50A (top), and the energy kick to ions in the kicker section for ions with various longitudinal and horizontal positions (bottom left) and for ions with zero horizontal position (bottom right).

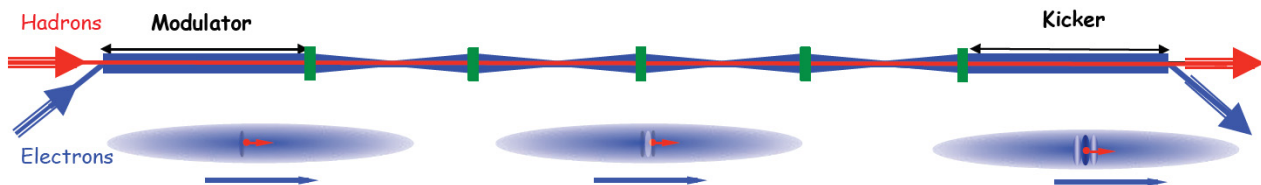


Figure 2: Schematic of a CeC system with the PCA.

* Work supported by Brookhaven Science Associates, LLC under Contract No. DE-SC0012704 with the U.S. Department of Energy.

[†] jma1@bnl.gov

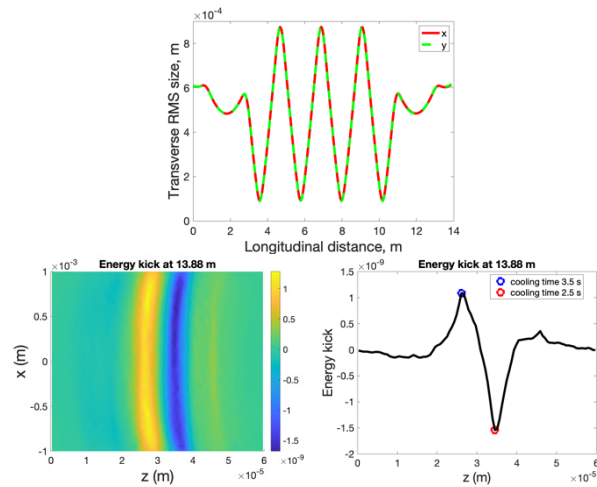


Figure 3: Evolution of transverse RMS beam size in a 4-cell-PCA based CeC system for electron beam peak current 75A (top), and the energy kick to ions in the kicker section for ions with various longitudinal and horizontal positions (bottom left) and for ions with zero horizontal position (bottom right).

Figures 1 and 3 show the electron beam size evolution in the PCA-based CeC system for the two cases listed in Table 1, and the energy kick to hadrons in the kicker section. The energy kick from the electrons corrects the hadrons' energy towards the nominal value, which results in the cooling. Both cases provide sufficient energy kick to hadrons and result in reasonable local cooling time, as can be seen in Figures 2 and 3. More simulations of the modulator and the PCA can be found in [9-18].

PCA WITH ORBIT DEVIATION

We have simulated the electron beam dynamics through the PCA to explore the effect of orbit deviation on the PCA gain. A transverse orbit deviation of 0.25 mm has been introduced at the entrance of the PCA. We have tracked the PCA gain and compared the cases of orbit correction at different locations along the beam line. Such comparison is presented in Figure 4. The last row in Figure 4 shows that the initial orbit deviations will be amplified in the PCA without orbit correction, which significantly reduces the PCA gain. The earlier we correct the orbit, the more we can restore the PCA gain. With orbit correction at the 1st cell of PCA (2nd row in Figure 4), the PCA gain is as large as that without orbit deviation (1st row in Figure 4).

The correlation between the increased orbit deviation and the reduced PCA gain has been explored by tracking a longitudinal slice of electrons. As can be seen in Figure 5, we have compared three cases of initial orbit deviation 0 mm, 0.1 mm and 0.25 mm, and found that orbit deviation can cause mismatch of transverse beam size in the designed PCA lattice. In each of the three cases, we tracked the dynamics of a longitudinal slice of electrons, which are shown in Figure 6.

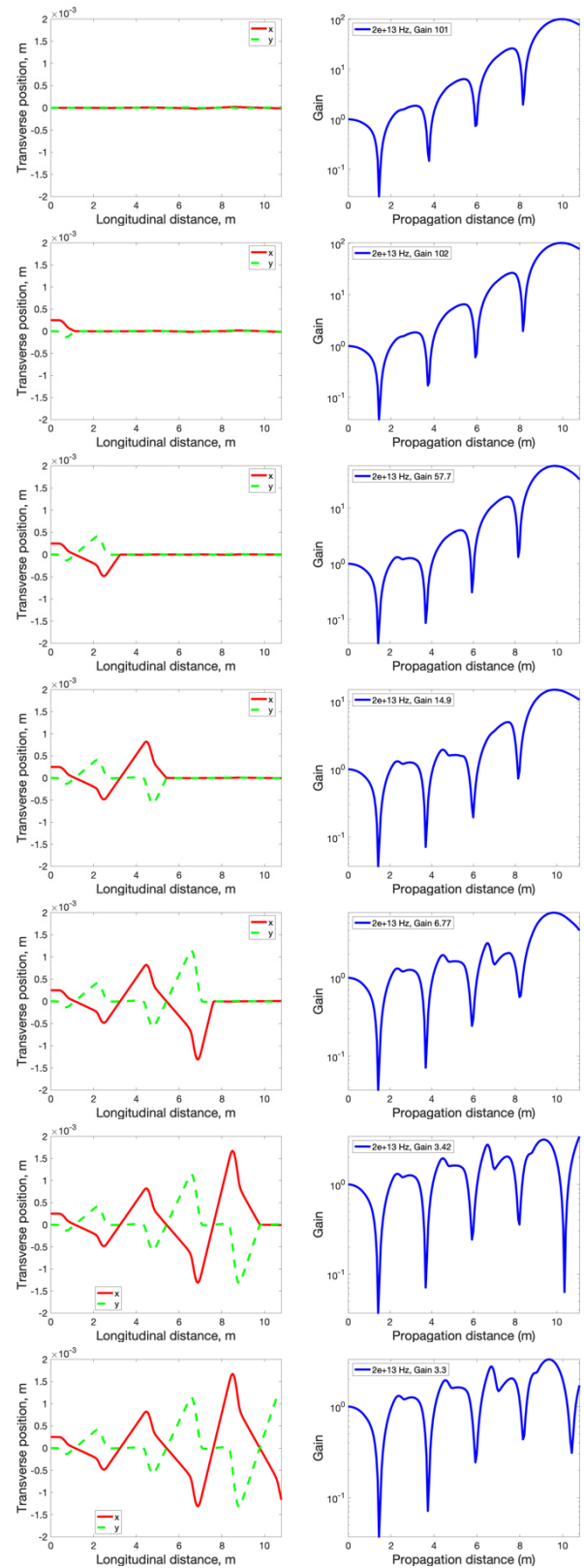


Figure 4: Evolution of transverse beam position in a 4-cell PCA (left column) and corresponding PCA gain at $2e+13$ Hz (right column) for electron beam without orbit deviation (1st row), with initial orbit deviation 0.25 mm and orbit correction at 1st PCA cell (2nd row), 2nd PCA cell (3rd

row), 3rd PCA cell (4th row), 4th PCA cell (5th row), exit of PCA (6th row), and without orbit correction (7th row).

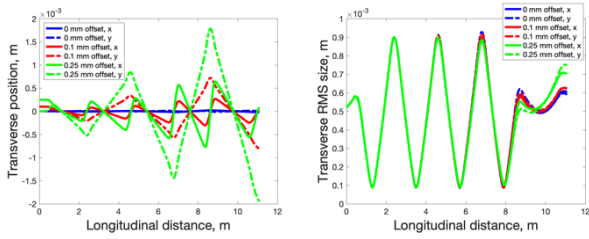


Figure 5: Evolution of transverse beam position (left) and transverse RMS beam size (right) in a 4-cell PCA for electron beam with initial transverse orbit deviation 0 mm (blue), 0.1 mm (red) and 0.25 mm (green).

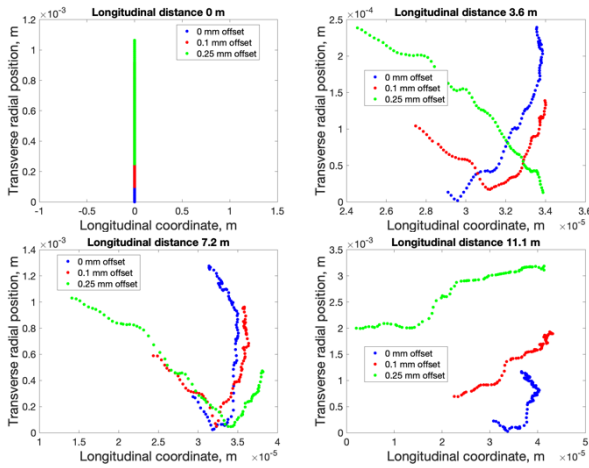


Figure 6: Dynamics of a longitudinal slice of electrons in a 4-cell PCA for electron beam with initial transverse orbit deviation 0 mm (blue), 0.1 mm (red) and 0.25 mm (green). The transverse radial position is defined as $r = \sqrt{x^2 + y^2}$.

Figure 6 shows that electrons with larger orbit deviation will spread more in longitudinal coordinate in PCA. The reason of the longitudinal spread is that electrons with larger orbit deviation are kicked by stronger transverse magnetic field of the solenoids, which results in more longitudinal spread. Such spread plays a similar role in PCA gain reduction as energy spread [18].

CEC WITH ORBIT DEVIATION

We have included the orbit deviation in the CeC simulations to study its effect on the cooling performance. In this study, we have used the beam parameters listed as Case 1 in Table 1. Instead of the initial orbit deviation, we have applied the vertical magnetic field $1e-5$ T in the CeC beam line, which is based on the measurement of the earth magnetic field at the location of the CeC system at BNL RHIC.

Figure 7 shows that the earth magnetic field causes orbit deviation and mismatch of beam size in the PCA-based CeC lattice, which degrade the cooling performance. The correctors in the CeC beam line have been utilized to correct the orbit, and the resulting orbit is shown in Figure 8. The locations of the correctors are based on the CeC system at BNL RHIC. The comparison between Figure 8 and

Figure 2 shows that the orbit correction restores the cooling performance.

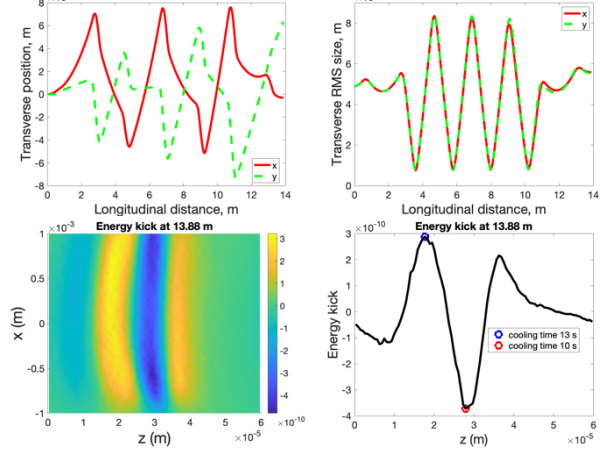


Figure 7: Evolution of transverse beam position (top left), transverse RMS beam size (top right) in a 4-cell-PCA based CeC system for electron beam peak current 50A with earth magnetic field, and the energy kick to ions in the kicker section for ions with various longitudinal and horizontal positions (bottom left) and for ions with zero horizontal position (bottom right).

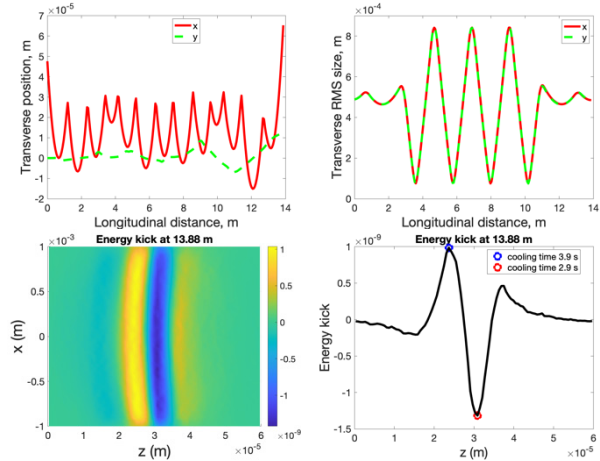


Figure 8: Evolution of transverse beam position (top left), transverse RMS beam size (top right) in a 4-cell-PCA based CeC system for electron beam peak current 50A with earth magnetic field and orbit correction, and the energy kick to ions in the kicker section for ions with various longitudinal and horizontal positions (bottom left) and for ions with zero horizontal position (bottom right).

CONCLUSION

We have simulated proper electron beam parameters which will provide good cooling performance in the PCA-based CeC system. The orbit deviation and earth field have been included in the simulations, which lead to worse cooling performance. We have demonstrated that the cooling performance can be restored with proper orbit correction.

REFERENCES

- [1] Y. S. Derbenev and V. N. Litvinenko, “FELs and High-energy Electron Cooling”, in *Proc. FEL'07*, Novosibirsk, Russia, Aug. 2007, paper TUCAU01, pp. 268-275.
- [2] V. N. Litvinenko, “Coherent Electron Cooling”, in *Proc. PAC'09*, Vancouver, Canada, May 2009, paper FR1GRI01, pp. 4236-4240.
- [3] V. N. Litvinenko and Y. S. Derbenev, “Coherent Electron Cooling”, *Phys. Rev. Lett.*, vol. 102, p. 114801, Mar. 2009. doi:10.1103/PhysRevLett.102.114801
- [4] V. N. Litvinenko *et al.*, “Plasma-Cascade Micro-Bunching Amplifier and Coherent Electron Cooling of a Hadron Beams”, 2018. arXiv:1802.08677
- [5] V. N. Litvinenko *et al.*, “Plasma-Cascade Instability”, *Phys. Rev. ST Accel. Beams*, vol. 24, p. 014402, Jan. 2021. doi:10.1103/PhysRevAccelBeams.24.014402
- [6] V. N. Litvinenko *et al.*, “Plasma-Cascade Instability- Theory, Simulations and Experiment”, 2019. arXiv:1902.10846
- [7] K. Yu and R. Samulyak, “SPACE Code for Beam-Plasma Interaction”, in *Proc. IPAC'15*, Richmond, VA, USA, May 2015, pp. 728-730. doi:10.18429/JACoW-IPAC2015-MOPMN012
- [8] J. Ma *et al.*, “Simulation of Beam-induced Plasma for the Mitigation of Beam-Beam Effects”, in *Proc. IPAC'15*, Richmond, VA, USA, May 2015, pp. 734-736. doi:10.18429/JACoW-IPAC2015-MOPMN015
- [9] J. Ma *et al.*, “Simulation Studies of Modulator for Coherent Electron Cooling”, *Phys. Rev. ST Accel. Beams*, vol. 21, p. 111001, Nov. 2018. doi:10.1103/PhysRevAccelBeams.21.111001
- [10] J. Ma, “Numerical Algorithms for Vlasov-Poisson Equation and Applications to Coherent Electron Cooling”, Ph.D. thesis, Department of Applied Mathematics and Statistics, Stony Brook University, Stony Brook, New York, USA, 2017.
- [11] J. Ma, G. Wang, and V. N. Litvinenko, “Simulations of Modulator for Coherent Electron Cooling”, in *Proc. IPAC'18*, Vancouver, Canada, Apr.-May 2018, pp. 2953-2956. doi:10.18429/JACoW-IPAC2018-THPAF005
- [12] J. Ma *et al.*, “Modulator Simulations for Coherent Electron Cooling”, in *Proc. NAPAC'16*, Chicago, IL, USA, Oct. 2016, pp. 816-819. doi:10.18429/JACoW-NAPAC2016-WEPOA55
- [13] J. Ma, G. Wang, and V. N. Litvinenko, “Simulations of Coherent electron Cooling with Two Types of Amplifiers”, *Int. J. Mod. Phys. A*, vol. 34, no. 36, p. 1942029, Dec. 2019. doi:10.1142/S0217751X19420296
- [14] J. Ma, G. Wang, and V. N. Litvinenko, “3D Start-to-End Simulations of the Coherent Electron Cooling”, in *Proc. IPAC'19*, Melbourne, Australia, May 2019, pp. 3329-3332. doi:10.18429/JACoW-IPAC2019-WEPTS092
- [15] J. Ma, G. Wang, and V. N. Litvinenko, “Simulations of Coherent electron Cooling with Free Electron Laser Amplifier and Plasma-Cascade Micro-Bunching Amplifier”, in *Proc. ICAP'18*, Key West, Florida, USA, Oct. 2018, pp. 52-58. doi:10.18429/JACoW-ICAP2018-SUPAF06
- [16] J. Ma, G. Wang, and V. N. Litvinenko, “Simulations of Cooling Rate and Diffusion for Coherent Electron Cooling Experiment”, in *Proc. IPAC'18*, Vancouver, Canada, Apr.-May 2018, pp. 2957-2960. doi:10.18429/JACoW-IPAC2018-THPAF006
- [17] J. Ma, G. Wang, and V. N. Litvinenko, “Simulations of Cooling Rate for Coherent Electron Cooling with Plasma Cascade Amplifier”, in *Proc. IPAC'21*, Campinas, SP, Brazil, May 2021, pp. 3261-3264. doi:10.18429/JACoW-IPAC2021-WEPAB265
- [18] J. Ma, G. Wang, and V. N. Litvinenko, “Simulation Studies of Plasma Cascade Amplifier”, in *Proc. IPAC'21*, Campinas, SP, Brazil, May 2021, pp. 3265-3268. doi:10.18429/JACoW-IPAC2021-WEPAB266